Society For Biomaterials

Corrosion of Mg alloy AZ91D in the presence of living cells

F. Seuss,[1] S. Seuss,[1]* M. C. Turhan,[1] B. Fabry,[2] S. Virtanen[1]

[1]Department of Materials Science and Engineering, WW4-LKO, University of Erlangen-Nuremberg, Martensstraβe 7, 91058 Erlangen, Germany
[2]Department of Physics, Biophysics, Center for Medical Physics and Technology, University of Erlangen-Nuremberg, Erlangen, Germany

Received 14 March 2011; revised 2 May 2011; accepted 8 May 2011
Published online 28 June 2011 in Wiley Online Library (wileyonlinelibrary.com). DOI: 10.1002/jbm.b.31896

Abstract: Mg and Mg alloys are of interest for biodegradable implants as they readily corrode in biological fluids, and dissolved Mg ions are nontoxic. Even though it is well known that Mg dissolution leads to pH increase in the surroundings, the effect of the corrosion-induced alkalization on the biological environment has not been studied in detail. We therefore explored the interactions between corrosion-induced pH increase and cell growth on Mg alloy AZ91D surface. Cell adhesion and spreading on the alloy surface is unimpeded initially. However, with time a large fraction of cells de-adhere. We attribute this to the observed increase of the pH in the cell culture medium in the process of alloy dissolution. Cytotoxicity tests with HeLa cells grown on glass surfaces confirm that cell death increases with increasing alkalinity of the cell culture medium. We also show that a the cells that adhere on the Mg alloy surface act as a corrosion-blocking surface layer. In consequence, a slower pH increase in the medium takes place when the alloy surface is covered with cells. Electrochemical impedance spectroscopy measurements (EIS) verify that a cell layer slows down the corrosion process. © 2011 Wiley Periodicals, Inc. J Biomed Mater Res Part B: Appl Biomater 99B: 276–281, 2011.

Key Words: magnesium alloy, cytotoxicity, pH, HeLa cells, electrochemical impedance spectroscopy

How to cite this article: Seuss F, Seuss S, Turhan MC, Fabry B, Virtanen S. 2011. Corrosion of Mg alloy AZ91D in the presence of living cells. J Biomed Mater Res Part B 2011:99B:276–281.

INTRODUCTION

Mg alloys have long been considered for use as biodegradable implant materials,[1–7] but it is still difficult to control the degradation (corrosion) rate of Mg alloys in the physiologic environment of an organism such that the desired structural and mechanical properties of the implant are maintained over a desired time window. On the basis of use of Mg alloys in other type of applications, many facts are known about Mg corrosion, such as the alkaline pH shift of a surrounding electrolyte, corrosion resistance in different types of inorganic electrolytes, or effects of alloy composition and microstructure on dissolution rates and modes.[8–10] Yet the influence of biomolecules or living cells on the corrosion behavior of Mg alloys *in vitro* or *in vivo* is not well understood (see[11] for a review). The converse question regarding the influence of Mg corrosion and corrosion products on cell function, although it has been recently addressed in numerous *in vitro* cell culture studies,[12–23] is also not yet answered to satisfaction. Materials, cell lines, and methods vary considerably between different studies, and it is difficult to draw general conclusions on the critical factors of cell adhesion and survival.

Even though the alkaline pH shift in the vicinity of corroding Mg surfaces is well known, the effect of this has not been systematically studied in view of the biomedical application of Mg. Therefore, one aim of the present investigation is the elucidation of Mg alloy corrosion-induced pH effects on biocompatibility. Generally, strong pH changes in cell culture medium are known to influence cell growth. For instance, maximum growth of HeLa cells and human liver cells cultured on glass was observed in the pH range of 7.38–7.87, followed by a gradual decline of cell growth at higher pH and an abrupt induction of cell death at a pH of 8.0–8.2.[24] Exposure time to higher pH also matters, as excessive cell death was observed when HeLa cells were exposed to alkaline pH of 7.8 for more than two days.[25]

Exposing magnesium alloys to simulated body fluids (SBF) or to cell culture medium, in spite of buffering, can lead to strong increase of the pH value far beyond the physiologic pH of 7.4.[19,26] Moreover, the pH development depends on many experimental parameters such as the alloy composition, buffering capacity of the medium, and alloy surface/medium volume ratio. But regardless of such details, impeded cell growth and induction of cell death can always be expected when cells are cultured on corroding Mg alloy surfaces.

In this study, the effect of alkaline pH shift in medium, caused by Mg alloy AZ91D corrosion, on cell adhesion, and

**Present address:* Department of Materials Science and Engineering, WW7-BioMat, University of Erlangen-Nuremberg, Cauerstraße 7, 91058 Erlangen, Germany.
Correspondence to: S. Virtanen; e-mail: virtanen@ww.uni-erlangen.de

TABLE I. Composition of AZ91D Cast Alloy

	Al	Zn	Mn	Si	Cu	Ni	Fe	Mg
wt %	8.5	0.6	0.25	0.005	0.25	0.001	0.004	balance

spreading on the alloy surface was investigated. In addition, the effect of cell adhesion layers on Mg alloy corrosion was studied by electrochemical impedance spectroscopy (EIS) measurements in absence and presence of cells on the surface. We chose the Mg alloy AZ91D for these investigations, as it is possible to culture cells on a corroding surface of this alloy (in contrast to commercially pure Mg, in which case the surface is too reactive for initial cell adhesion without surface treatments[19]). Moreover, the alloy AZ91D is one of the most used Mg-based alloys, with improved mechanical and corrosion behavior as compared to pure Mg. The corrosion behavior of AZ91D has been previously studied in simulated body fluids,[20,27,28] and *in vitro* cell culture testing on this alloy has also been carried out.[6,12]

MATERIALS AND METHODS

The Mg alloy used for the experiments was cast AZ91D, with the major alloying elements of approximately 9% Al and 1% Zn (for composition see Table I). The samples were cut from sheet material to a size of 1.75 × 1.75 cm^2, ground with 1200 SiC grinding paper, then polished with 6, 3, and finally 1-μm diamond paste and cleaned in an ultrasonic bath with ethanol. For pH measurements, an o-ring (Ø 0.8 cm) was attached to the surface, defining constant contact geometry between the sample and the electrolyte. For the measurement of the pH development, simulated body fluid SBF 5[29] was used (for composition, see Table II).

The pH development with time was studied with three different pretreatments of the samples. The samples were (a) either left untreated (bare), (b) they were incubated in Dulbecco's Modified Eagle's Medium (DMEM) with addition of 10% Fetal Bovine Serum and 100 U/mL and 100 U/mL Penicillin/Streptomycin as culture medium for 2 h at 37°C, to simulate the chemical effects that occur on the surface while growing cells on a sample (DMEM pretreatment), or (c) 300,000 HeLa cells were grown on the sample for 2 h. After these treatments, a tube was connected to the o-ring and filled with 10 mL SBF; then the pH change of the solution was measured with a pH-Meter (Knick 763 Multi Calimatic) for 24 h.

For cell culture experiments, the Mg samples were sterilized under UV irradiation with a wavelength of 260 nm. Cells from a human cervical cancer cell line (HeLa) were cultured in an incubator (5% CO_2, 37°C, 95% relative humidity) for different times (2–24 h) in 24-well plates containing the Mg alloy samples. About 300,000 cells were seeded on the surface. HeLa cells are a standard cell line used in many laboratories worldwide; they show robust growth under a range of conditions and form a dense monolayer when grown onto a flat substrate, which makes them suitable for cell attachment and spreading area quantification. Again DMEM, prepared as mentioned above, was used as a cell culture medium. After 2–24 h in the incubator, the cells were fixed in 2% paraformaldehyde and stained with Alexa red phalloidin to visualize the actin cytoskeleton of the cells, and with Hoechst 33342 to visualize the cell nucleus. Fluorescence microscopy of the stained cells was carried out with a Leica CTR 6000 model microscope. A minimum of three samples was measured for each condition. For each sample, images recorded with a 10× objective from at least three randomly chosen field of views were analyzed.

To examine the influence of increasing pH value on the cell behavior, DMEM was alkalized with 0.1 molar $NaOH_{(aq)}$. Solutions with pH values of 7.4, 8.0, 9.0, 10.0, and 11.5 were prepared. For each experiment, 100,000 cells were seeded on glass, and cultured for 24 h in an incubator. Fixation, staining and fluorescence microscopy was carried out as explained above.

To evaluate the influence of a cells layer on the corrosion behavior of AZ91D, 100,000 or 300,000 HeLa cells were cultured for 2 h or 5 h on UV irradiated AZ91D samples as described above. Afterwards, the samples were transferred to SBF 5 medium and analyzed at 37°C with EIS using an electrochemical workstation (IM6ex, Zahner Elektronik, Germany). The frequency of the measurements ranged between 10 mHz and 100 kHz, at an amplitude of 10 mV. All EIS measurements were performed at the open circuit potential (OCP). For comparison, only pretreated samples within 200 μL of DMEM culture medium for two hours were tested. It is known that pretreatment with DMEM causes the formation of a passivation layer on the sample surface.[30]

RESULTS AND DISCUSSION

pH development in SBF

The pH in the medium increased with time for all AZ91D samples, with the polished samples showing the fastest increase and the sample with the cell layer showing the slowest increase (Figure 1). Scanning Electron Microscopy/Energy Dispersive X-ray Spectroscopy (SEM/EDX) measurements of AZ91D samples pretreated with culture medium revealed partial, inhomogeneous coverage of the surface with a carbonated calcium phosphate layer (data not shown). This layer partially blocks the dissolution of the

TABLE II. Composition of Simulated Body Fluid (SBF 5) Used in This Study in Comparison With Human Blood Plasma[29]

Ion	Na^+	K^+	Mg^{2+}	Ca^{2+}	Cl^-	H_3CO^-	HPO_4^{2-}	SO_4^{2-}
Plasma	142.0	3.6–5.5	1.0	2.1–2.6	95.0–107.0	27.0	0.65–1.45	1.0
SBF5	142.0	5.0	1.0	2.5	131.0	5.0	1.0	1.0

Concentrations are given in mmol/L.

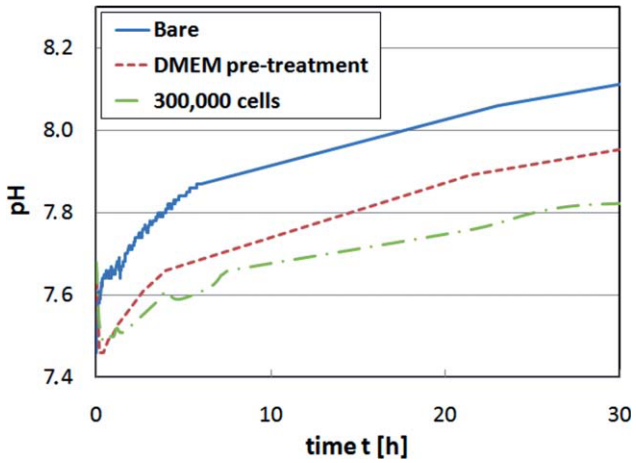

FIGURE 1. pH-development of differently treated AZ91D samples in SBF as a function of time. [Color figure can be viewed in the online issue, which is available at wileyonlinelibrary.com.]

sample, and therefore limits the pH increase by reducing the size of the effective surface. With additionally cells attached, the freely exposed surface is even smaller; consequently the pH increase is less pronounced. These results suggest that a cell layer acts as a kinetic barrier against dissolution and therefore plays an important role for corrosion-induced pH changes.

Cytotoxicity in dependence of pH value in medium

Figure 2 shows the effect of the pH of the culture medium on HeLa cells grown on glass. The cell density decreases with increasing pH of the medium. The effect was gradual, however, and even at a very high pH of 10 we observed that a considerable fraction of the cells remained attached to the alloy surface. A dramatic decline of the cell density and spreading area was only observed at pH $>$ 10, suggesting that cells are not viable under these conditions.

Cell density and spreading on the Mg alloy AZ91D

Figure 3 shows the time dependence of cell density on AZ91D. In the first 5 h of culture, the cell density on the alloy surface remains constant (Figure 3). In this time period, we observe even an increase in the cell spreading area, which indicates that the cells are viable and function normally. After 8 h, cell density has dropped to about 30–35% of the initial

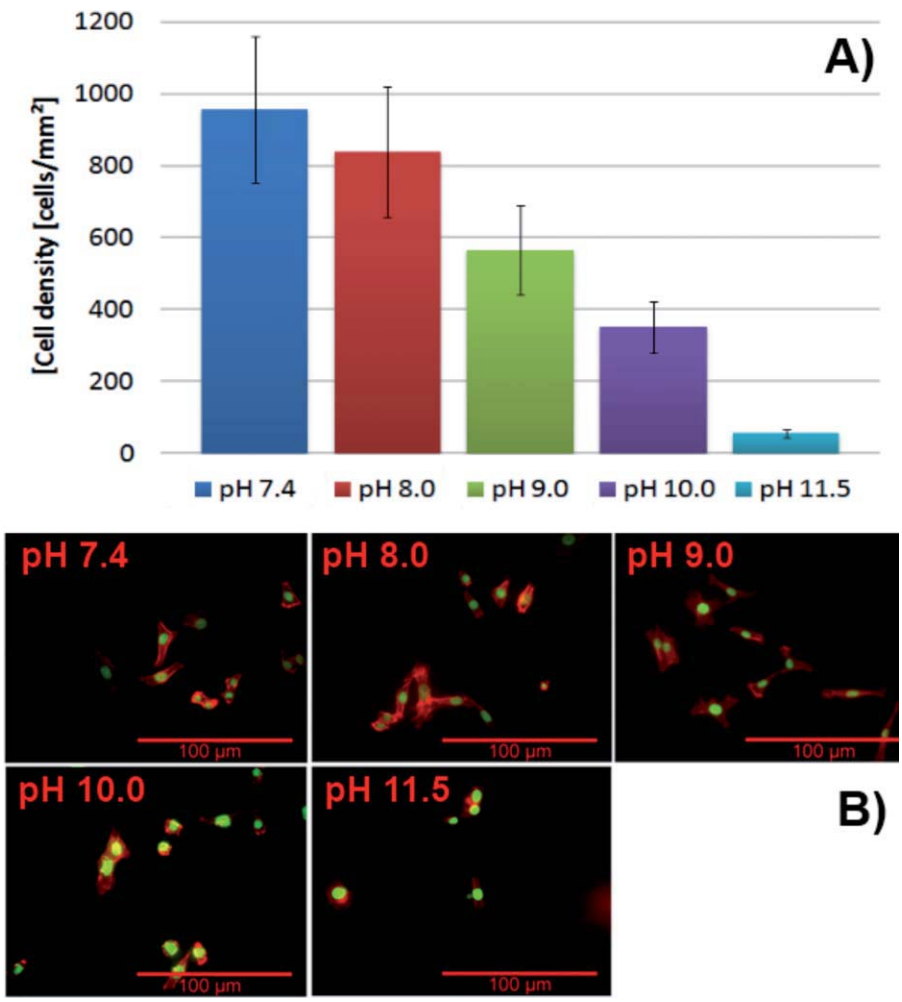

FIGURE 2. A: Density of HeLa cells cultured on glass for 24 h as a function of the pH value of the culture medium. B: Cell spreading of HeLa cells on glass at different pH values. [Color figure can be viewed in the online issue, which is available at wileyonlinelibrary.com.]

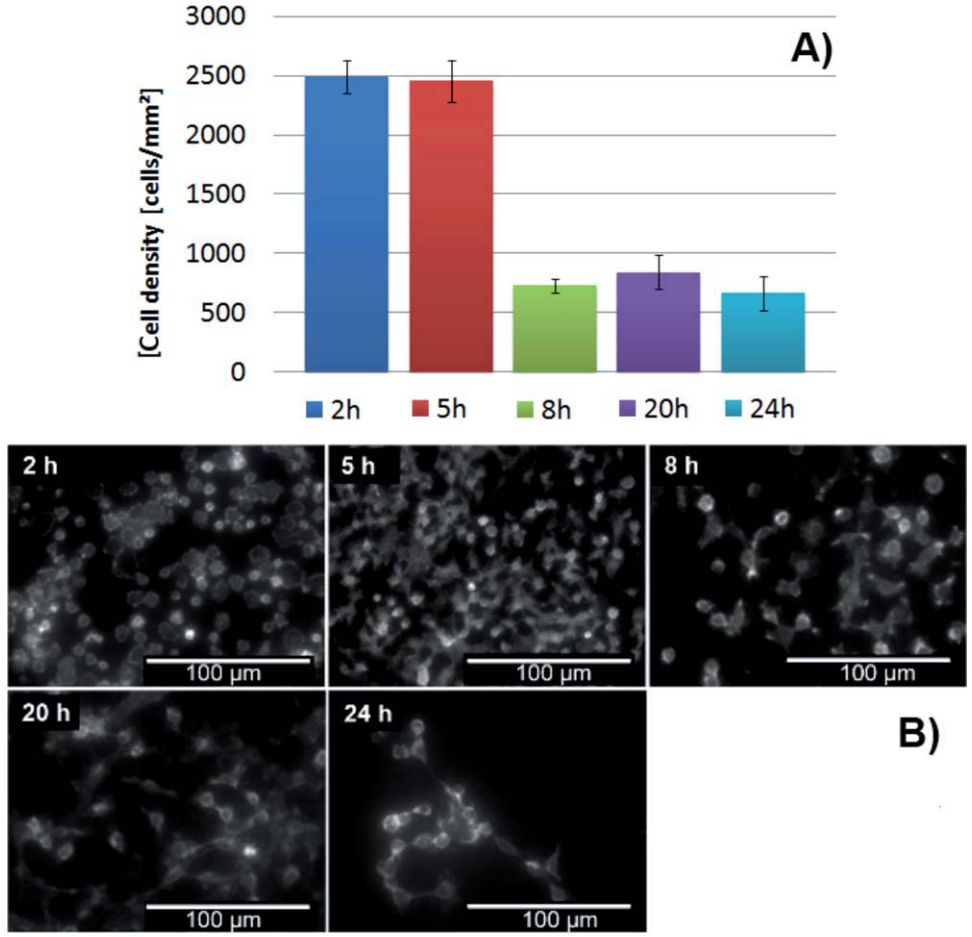

FIGURE 3. A: Density of cells grown on AZ91D as a function of time. B: Actin staining of HeLa cells grown on AZ91D for 2, 5, 8, 20, and 24 h. [Color figure can be viewed in the online issue, which is available at wileyonlinelibrary.com.]

value. Many cells show a spherical shape. For the final 16 h of the experiment, the cell density remains approximately constant but low, and most cells show a spherical shape.

The 8-h time point at which cell density declined drastically cannot be explained with an excessive pH of the medium (Figure 1). Rather, we speculate that the local pH at the interface between the alloy surface and the cell layer was substantially higher than in the bulk of the medium. Nevertheless, a substantial fraction of cells (30%) can survive for one day on corroding AZ91D surface. A locally high pH at the cell-material interface can contribute to a further passivation of the alloy surface and may explain why the pH increase in the bulk of the medium was substantially slower compared with untreated samples (Figure 1).

Electrochemical impedance spectroscopy

The hypothesis of a cell-layer induced passivation was further investigated with electrochemical impedance spectroscopy. Previously, electrochemical measurements in the presence of cells on surfaces have been carried out on passive materials such as Ti alloys or stainless steels.[31–35] Typically, an increase of the polarization resistance as determined by impedance spectroscopy is observed in the presence of cells on the material surface. These effects were explained by an additional resistance over the metal/electrolyte-interface that is introduced by the cell layer. However, as the impedance of passive metals is several orders of magnitude higher than the resistance through the cell adhesion layer, the influence of cells is not very well visible in such measurements. In contrast to these previous measurements on passive metals, due to the high electrochemical activity of

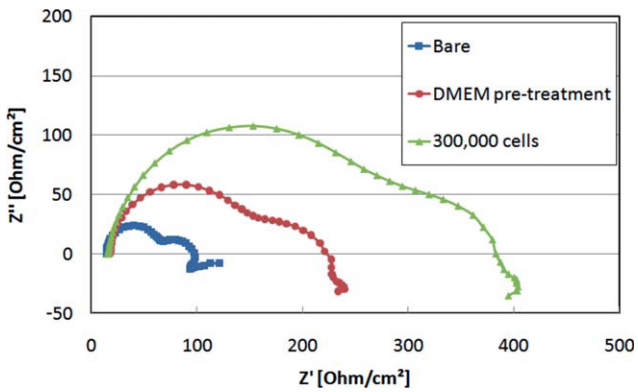

FIGURE 4. Nyquist plots of the electrochemical impedance spectra of AZ91D samples (untreated, pretreated with DMEM, and with cells after 2 h of culture) in simulated body fluid at 37°C. [Color figure can be viewed in the online issue, which is available at wileyonlinelibrary.com.]

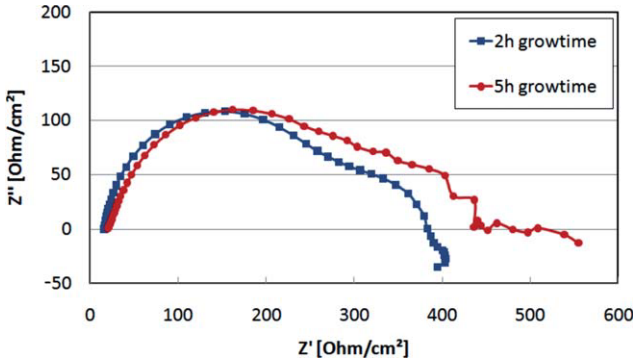

FIGURE 5. Nyquist plot of the electrochemical impedance spectra of AZ91D samples with cells in simulated body fluid at 37°C at different culture times. [Color figure can be viewed in the online issue, which is available at wileyonlinelibrary.com.]

magnesium alloys, the charge transfer resistance values are several orders of magnitude lower than for passive metals, and hence surface blocking effects by the cell layers are expected to become very clearly visible.

EIS spectra of different AZ91D samples were recorded and the Nyquist plots for these samples are shown in Figures 4 and 5. In the Nyquist plots, two capacitive loops with an inductive loop are observed for all samples, similar to previously reported data on pure Mg[36–39] and on the AZ91D alloy.[40] Most strikingly, the impedance was highest on the samples covered with a cell layer. This result is in support of our hypothesis of a cell-layer induced passivation and suggests that a cell layer increases the charge transfer resistance either directly or indirectly by stabilizing or supporting the formation of a chemical passivation layer at the alloy surface.

Sample pre-treatment by incubation in cell culture medium, however, also leads to an increased charge transfer resistance (Figure 4), consistent with an earlier report of a strong decrease of the corrosion rate of pure Mg upon incubation of the sample in cell culture medium.[30] It is therefore important to separate the effect of cell growth from the effect of the cell culture medium. We observed a further increase in the impedance with longer cell culture time of 5 h (Figure 5), consistent with the better cell spreading at

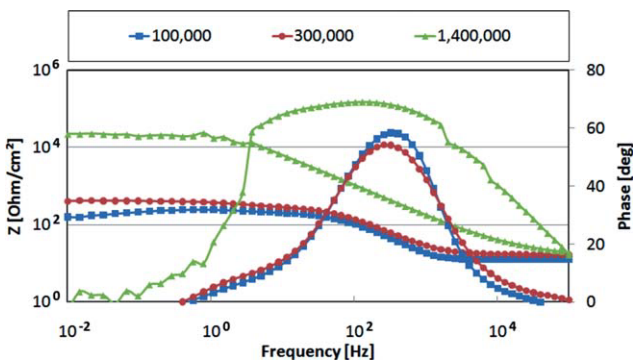

FIGURE 6. Bode plot of electrochemical impedance spectra of AZ91D samples in simulated body fluid at 37°C for different initial cell seeding densities. [Color figure can be viewed in the online issue, which is available at wileyonlinelibrary.com.]

this time point (Figure 3a). Moreover, a higher number of cells initially seeded on the surface leads to a larger increase of the impedance (Figure 6). A presentation of the impedance spectra as Bode plot (Figure 6) indicates a shift of the interfacial capacitance in presence of cells; this effect is especially noteworthy in the case of the highest number of cells seeded on the surface. The increased charge transfer resistance as well as the shift of the interfacial capacitance indicate that the cell adhesion layer may not only act as a physical barrier for electrochemical reactions by partially blocking the electrochemically active surface, but that the cells may have altered the chemical composition of the Mg alloy surface towards a more corrosion resistant passivation layer. To test this possibility in future studies, we propose to measure the changes in the impedance spectra after proteolytic removal of the cells from the alloy surface. Bode plot was chosen because of the big difference of the transfer resistance and the benefits of a logarithmic scale in this case.

CONCLUSIONS

Adhesion and spreading of HeLa cells on AZ91D magnesium alloy is possible but limited by the ongoing corrosion process, foremost due to an alkaline pH shift in the medium. During Mg alloy corrosion, the pH in the vicinity of the sample surface is increased, but the pH increase in the medium is significantly smaller when cells were present. Electrochemical impedance spectroscopy showed higher impedances for samples with an adherent cells layer that acts as a physical barrier and slows down the electrochemical reactions during corrosion.

REFERENCES

1. Heublein B, Rohde R, Kaese V, Niemeyer M, Hartung W, Haverich A. Biocorrosion of magnesium alloys: A new principle in cardiovascular implant technology? Heart 2003;89:651–656.
2. Peuster M, Beerbaum P, Bach F-W, Hauser H. Are resorbable implants about to become a reality? Cardiol Young 2006;16: 107–116.
3. Staiger MP, Pietak AM, Huadmai J, Dias G. Magnesium and its alloys as orthopedic biomaterials: A review. Biomaterials 2006;27: 1728–1734.
4. Song G. Control of biodegradation of biocompatible magnesium alloys. Corrosion Sci 2007;49:1696–1701.
5. Von Der Höh N, Bormann D, Lucas A, Denkena B, Hackenbroich C, Meyer-Lindenberg A. Influence of different surface machining treatments of magnesium-based resorbable implants on the degradation behavior in rabbits. Adv Eng Mater 2009;11:B47–B54.
6. Witte F, Fischer J, Nellesen J, Crostak H-A, Kaese V, Pisch A, Beckmann F, Windhagen H. In vitro and in vivo corrosion measurements of magnesium alloys. Biomaterials 2006;27:1013–1018.
7. Staiger M P, Pietak A M, Huadmai J, Dias G. Magnesium and its alloys as orthopedic biomaterials: A review. Biomaterials 2006;27: 1728–1734.
8. Song G, Atrens A. Corrosion mechanisms of Mg alloys. Adv Eng Mater 1999;1:11–33.
9. Atrens A, Song G. Understanding magnesium corrosion. A framework for improved alloy performance. Adv Eng Mater 2003;5: 837–858.
10. Song G, Atrens A. Recent insights into the mechanism of magnesium corrosion and research suggestions. Adv Eng Mater 2007;9: 177–183.
11. Witte F, Hort N, Vogt C, Cohen S, Kainer KU, Willumeit R, Feyerabend F. Degradable biomaterials based on magnesium corrosion. Current Opin Solid State Mater Sci 2008;12:68–72.

12. Witte F, Feyerabend F, Maier P, Fischer J, Störmer M, Blawert C, Dietzel W, Hort N. Biodegradable magnesium-hydroxyapatite metal matrix composites. Biomaterials 2007;28: 2163–2174.
13. Zhang Y, Tao H-R, He Y-H, Zou G-Y, Jiang Y, Zhang S-X, B.-L, Zhang B-L, Li J-N, Zhao C-L, Zhang X-N. Cytotoxicity and hemolytic properties of biodegradable Mg-Zn alloy. J Clin Rehabilitative Tissue Eng 2008;12:8162–8166.
14. Gu X, Zheng Y, Cheng Y, Zhong S, Xi T. In vitro corrosion and biocompatiblity of binary magnesium alloys. Biomaterials 2009; 30:484–498.
15. Zhang E, Yin D, Xu L, Yang L, Yang K. Microstructure, mechanical and corrosion properties and biocompatibility of Mg-Zn-Mn alloys for biomedical application. Mater Sci Eng C 2009;29:987–993.
16. Zhang S, Li J, Song Y, Zhao C, Zhang X, Xie C, Zhang Y, Tao H, He Y, Jiang Y, Bian Y. In vitro degradation, hemolysis and MC3T3-E1 cell adhesion of biodegradable Mg-Zn alloy. Mater Sci Eng C 2009;29:1907–1912.
17. Yun Y, Dong Z, Yang D, Schulz MJ, Shanov VN, Yarmolenko S, Xu Z, Kumta P, Sfeir C. Biodegradable Mg corrosion and osteoblast cell culture studies. Mater Sci Eng C 2009;29:1814–1821.
18. Gu XN, Zheng W, Cheng Y, Zheng YF. A study on alkaline heat treated Mg-Ca alloy for the control of the biocorrosion rate. Acta Biomaterialia 2009;5:2790–2799.
19. Lorenz C, Brunner JG, Kollmannsberger P, Jaafar L, Fabry B, Virtanen S. Effect of surface pre-treatments on biocompatibility of magnesium. Acta Biomaterialia 2009;5:2783–2789.
20. Zhang Y, Tao H-R, He Y-H, Jiang Y, Zhang S-X, Zhang X-N. Effect of Mg-Zn alloy on integrin beta-1 expression in osteoblasts. J Clin Rehab Tissue Eng Res 2009;13:7531–7534.
21. Yun Y, Dong Z, Yang D, Shanov V, Yarmolenko S, Xu Z, Kumta P, Sfeir C, Doepke A, Schulz M. Biodegradable Mg for bone implants: Corrosion and osteoblast culture studies. ASME Int Mech Eng Cong Exposition Proc 2009;15:125–129.
22. Gu X, Zheng Y, Zhong S, Xi T, Wang J, Wang W. Corrosion of, and cellular responses to Mg-Zn-Ca bulk metallic glasses. Biomaterials 2010;31:1093–1103.
23. Xin Y, Jiang J, Huo K, Tang G, Tian X, Chu P K. Corrosion resistance and cytocompatibility of biodegradable surgical magnesium alloy coated with hydrogenated amorphous silicon. J Biomed Mater Res A 2009;89:717–726.
24. MacKenzie CG, MacKenzie JB, Beck P. The effect of pH on growth, protein synthesis, and lipid-rich particles of cultured mammalian cells. J Biophys Biochem Cytol 1961;9:141–156.
25. Barton ME. Effect of pH on the growth cycle of HeLa cells in batch suspension culture without oxygen control. Biotechnol Bioeng 1971;13:471–492.
26. Quach N-C, Uggowitzer P J, Schmutz P. Corrosion behavior of an Mg-Y-RE alloy used in biomedical applications studied by electrochemical techniques. Comptes Rendus Chimie 2008;11:1043–1054.
27. Xin Y, Liu C, Zhang X, Tang G, Tian X, Chu P K. Corrosion behavior of biomedical AZ91D magnesium alloy in simulated body fluids. J Mater Res Mater Res Soc 2007;22:2004–2011.
28. Xin Y, Hu T, Chu PK. Influence of test solutions on in vitro studies of biomedical magnesium alloys. J Electrochem Soc 2010;157: C238–C243.
29. Müller L, Müller FA. Preparation of SBF with different HCO3- content and its influence on the composition of biomimetic apatites. Acta Biomateralia 2006;2:181–189.
30. Keim S, Brunner J G, Fabry B, Virtanen S. Control of magnesium corrosion and biocompatibility with biomimetic coatings. J Biomed Mater Res Part B Appl Biomater B 2011;96:84–90.
31. Hiromoto S, Noda K, Hanawa T. Development of electrolytic cell with cell-culture for metallic biomaterials. Corrosion Sci 2002;44: 955–965.
32. Hiromoto S, Noda K, Hanawa T. Electrochemical properties of an interface between titanium and fibroblasts L929. Electrochimica Acta 2002;48:387–396.
33. Huang H-H. In situ surface electrochemical characterization of Ti and Ti-6Al-4V alloy cultured with osteoblast-like cells. Biochem Biophys Res Commun 2004;314:787–792.
34. Hiromoto S. Polarisation behavior of 316L stainless steel in cell culture environment. Mater Sci Forum 2007;561–565: 1459–1462.
35. Garcia-Alonso MC, Saldana L, Alonso C, Barranco V, Munoz-Morris MA, Escudero ML. In situ cell culture monitoring on a Ti-6Al-4V surface by electrochemical techniques. Acta Biomaterialia 2009;5:1374–1384.
36. Song G, Atrens A, Wu X, Zhang B. Corrosion behaviour of AZ21. AZ501 and AZ91 in Sodium Chloride. Corrosion Sci 1998;40: 1769–1791.
37. Mathieu S, Rapin C, Hazan J, Steinmetz P. Corrosion behaviour of high pressure die-cast and semi-solid cast AZ91D alloys. Corrosion Sci 2002;44:2737–2756.
38. Baril G, Pébère N. Corrosion of pure magnesium in aerated and deaerated sodium sulphate solutions. Corrosion Sci 2001;43: 471–484.
39. Baril G, Blanc C, Pébère NAC. Impedance spectroscopy in characterizing time-dependent corrosion of AZ91 and AM50 magnesium alloys: Characterization with respect to their microstructures. J Electrochem Soc 2001;148:b469–b496.
40. Turhan MC, Lynch R, Killian MS, Virtanen S. Effect of acidic etching and fluoride treatment on corrosion performance in Mg alloy AZ91D (MgAlZn). Electrochimica Acta 2009;55:250–257.